# Preserving half-metallic surface states in $CrO_2$: Insights into surface reconstruction rules

Bei Deng,[1] X. Q. Shi,[1,*] L. Chen,[1,†] and S. Y. Tong[1,2,‡]

[1]*Department of Physics, Southern University of Science and Technology, Shenzhen 518055, China*

[2]*School of Science and Engineering, the Chinese University of Hong Kong (Shenzhen), Shenzhen 518172, China*

(Received 27 November 2017; revised manuscript received 12 February 2018; published 4 April 2018)

The issue of whether the half-metallic (HM) nature of $CrO_2$ could be retained at its surface has been a standing problem under debate for a few decades, but until now is still controversial. Here, based on the density functional theory calculations we show, in startling contrast to the previous theoretical understandings, that the surfaces of $CrO_2$ favorably exhibit a half-metallic–semiconducting (SmC) transition driven by means of a surface electronic reconstruction largely attributed to the participation of the unexpected local charge carriers (LCCs), which convert the HM double exchange surface state into a SmC superexchange state and in turn, stabilize the surface as well. On the basis of the LCCs model, a new insight into the surface reconstruction rules is attained. Our novel finding not only provided an evident interpretation for the widely observed SmC character of $CrO_2$ surface, but also offered a novel means to improve the HM surface states for a variety of applications in spintronics and superconductors, and promote the experimental realization of the quantum anomalous Hall effect in half-metal based systems.

DOI: 10.1103/PhysRevB.97.165404

## I. INTRODUCTION

Well known as an important double-exchange half-metallic (HM) ferromagnet, chromium dioxide ($CrO_2$) inherently has a fully spin-polarized nature around the Fermi level, which gives rise to a wide range of potential applications in spintronics and magnetoelectronics [1–3]. The HM feature of $CrO_2$ was first discovered by band structure calculations in 1980s [4], and later thoroughly understood by a local spin-density approximation (LSDA) taking into consideration of the Hubbard $U$ correction [5], which demonstrated that the electron correlation is a crucial term accounts for the observed HM states and in turn explained why $CrO_2$ is not a Mott insulator. Although the research of $CrO_2$ has undergone a long history of more than three decades, recently, this traditional transitional-metal dioxide has again received growing attention due to the experimental/theoretical demonstrations of its potential applications in superconducting spintronics [6–8], quantum anomalous Hall effect (QAHE) [9] as well as magnetic Weyl semimetals [10]. Given this set of exciting potential applications and long history, one would expect that the fundamental physics of this half-metal has been fully understood, with the associated mechanisms well addressed. On the contrary, up to now, there remains a lack of thorough understanding towards its very fundamental properties, among which the unclarified surface physics should be a typification.

In particular, the issue of whether this ferromagnetic half-metal could retain its half-metallicity on the surface has been a long standing problem under debate for more than two decades, but until now is still controversial. While it is well known that the $CrO_2$ is not stable in the air ambient and is readily decomposed into semiconducting (SmC) $Cr_2O_3$ phase, the HM surface states are difficult to be attained even by advanced techniques like chemical vapor depositions (CVD) [11–16], despite that lots of early theoretical perspectives suggested that the surfaces of $CrO_2$ are subject to a HM nature [17,18]. Meanwhile, a few groups were still able to observe a continued indication of HM characteristics at the surface by the very same approach [19–21]. To address such controversy, Hong and Che [22] proposed an interpretational mechanism based on density functional plane-wave method, suggesting that the $e_g$–$t_{2g}$ inversion could be a driving force for the observed SmC states on (001) surface. However, in a later report [18], they further pointed out that this mechanism is not applicable to surfaces of other orientations, for example, the (100) surface. While such a mechanism is fruitful to explain the SmC nature of (001) surface, still, not all the SmC surfaces are (001) orientated. Recently, based on the combined density functional theory and model theory, Cai *et al.* [9] have pointed out a possibility of realizing QAHE at $CrO_2$–$TiO_2$ interface. However, QAHE remains to be discovered despite that $CrO_2$ films are usually epitaxially grown on $TiO_2$ substrates. It can therefore be interpreted that (a) under the experimental conditions (like CVD approach widely employed to grow $CrO_2$), the surface and interfaces of $CrO_2$ cannot be as ideal HM as expected, and/or (b) the physics underlying the possible surface reconstructions remains to be fully understood. A more practical model and approach in tackling this surface/interface problem is largely needed.

In this paper, we consider the (100) surface as a prototypical example to probe the inherent surface/interface physics of $CrO_2$ and the associated HM–SmC transitions. Apart from the (001) surface, the (100)/(110) surfaces were also characterized to favor a SmC nature, but thus far little is known towards the inherent mechanism. Here, based on density functional plane-wave method we show, as for a complement and extension of the known surface physics of $CrO_2$, that the unexpected local

*shixq@sustc.edu.cn
†chenlang@sustc.edu.cn
‡tongsy@sustc.edu.cn

 

charge carriers (LCCs), consider, for example, the isolated H atoms, group VII anions, or group IA ions that may readily present in experiments [11–16], could be a driven factor that plays a key role in the breaking of the HM surface state. This finding also sheds light on the reason underlying the not-yet-discovered QAHE based on $CrO_2$–$TiO_2$ interface. Along with this finding, a new insight into the general rules on the thermodynamics and reconstructions of ionic crystal surfaces is then achieved. Accordingly, we have proposed an important guideline to overcome the difficulties in both the above respects. Therefore, our findings offer a crucial step towards the full application of $CrO_2$ as a HM ferromagnet in spintronics, and promote the realization of QAHE as well as other exotic properties in $CrO_2$-based systems.

## II. COMPUTATIONAL METHODS AND DETAILS

The study was performed on the basis of density functional theory, as implemented in the VASP code [23]. The local spin density approximation (LSDA) was adopted to acquire the geometric ground states as well as the spin-polarized electronic structure of $CrO_2$, while the PBE functional [24] was employed to deal with electron exchange-correlation. For the correlated $3d$ states of Cr, the rotationally invariant on-site Coulomb $U$ term, known as the LSDA+$U$ correction, was parameterized with 3 eV [25,26] for the Coulomb repulsive potential $U$ and 0.87 eV [25,26] for the intraorbital exchange potential $J$ as realized in the Liechtenstein implementation [27]. Projector-augmented wave (PAW) pseudopotentials [28] for O and Cr were used with a plane-wave basis-set cutoff energy of 420 eV. To simulate the surface, a vacuum slab which consists of eight atomic cation layers and 16 anion layers, with a vacuum space of 20 Å along the orientation, was constructed. The $9 \times 9 \times 14$ and $9 \times 14 \times 1$ Monkhorst-Pack meshes were used, respectively, for $k$-point samplings of the bulk and surface in their Brillouin zones. For geometric optimizations, all the atoms in the bulk/slab were allowed to relax until the calculated Hellmann-Feynman forces are less than $3 \times 10^{-3}$ eV/Å.

## III. THE SURFACE STATES OF O-TERMINATED $CrO_2$ (100) SURFACE

### A. The clean surface

It is possible for there to be three different terminations of $CrO_2$ (100) surface, as typified in Fig. 1, namely, O atom-terminated, double O atom-terminated and Cr atom-terminated cases, which are referred to hereafter as 100(O), 100(OO), and 100(Cr) surfaces, respectively. The ideal unrelaxed 100(O) surface is subject to Tasker's type II surface, which has one O-dangling bond together with one Cr-dangling bond. In $CrO_2$, the Cr atom is surrounded by six O atoms, which in turn form a slightly orthorhombic-distorted Cr–$O_6$ octahedral coordination, with each O atom coordinated with three Cr atoms. Hence, each Cr dangling bond carries 2/3 electrons ($e^-$) and each O dangling bond 2/3 holes ($e^+$). For the 100(O) surface, the two dangling bond will favorably exhibit compensation upon atomic relaxation. The surface Cr atoms will relax toward the [–1 1 0] direction, while the four O atoms (labeled by 1 and 2) surround it will relax backward, forming a distorted fivefold coordination, as depicted in Fig. 2(a) by the black arrows.

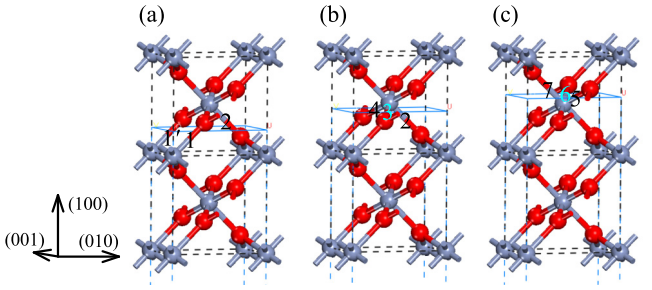


FIG. 1. Illustrated diagrams for (a) O-terminated, (b) OO-terminated, and (c) Cr-terminated (100) surfaces of $CrO_2$. The interpolated facets, which are enclosed by blue lines, display the three possible surface tops upon cleaving; the arabic numerals denote the dangling bonds for surfaces with different terminations, while 1' is a repeated image of dangling bond 1 due to the periodicity of the lattice geometry. The Cr and O atoms are represented by the light blue and red balls, respectively.

Given such surface morphology, we next examine its surface state by the projected electronic density of states (PDOS). The PDOS of the bulk $CrO_2$ and the relaxed 100(O) are given in Figs. 3(a)–3(b). For $CrO_2$, we notice that in comparison with the LSDA [29], the LSDA+$U$ yields somewhat flat and less localized $t_{2g}$ states near the Fermi level (which are isolated into lower lying $d_{xy}$, and higher lying $d_{yz\pm xz}$ due to the distortion of Cr–$O_6$ $O_h$), as typified in Fig. 3(a), indicating a moderately itinerant character of the $d_{yz\pm xz}$ states, which is in good agreement with the double-exchange model [30] and DMFT theory [31]. Here, we have also considered a hybrid density functional of HSE06 as an alternative of LSDA+U. In this respect, the HSE06 functional gives, however, a much more localized character of $t_{2g}$ and is therefore not adequate for this study. For the relaxed 100(O) surface, the $t_{2g}$ state is further splitted into several small peaks broadening around the Fermi level, due to the distortion of the fivefold Cr–$O_5$ square pyramid ($S_p$), yielding in agreement with Ref [5] gapless, almost flat density of states of the surface Cr atom, with the Fermi level situated in the middle, evidently confirming the metallic characteristic of the ideal $CrO_2$ (100) surface, as shown in Fig. 3(b). However, this is not compatible to explain the widely observed SmC feature.

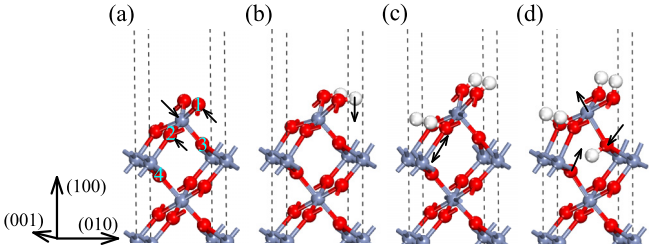


FIG. 2. The calculated surface geometries for the relaxed (a) 100(O), (b) 100(O)–H, (c) 100(O)–2H, and (d) 100(O)–3H surfaces. The arabic numerals label the O atoms that are favorably involved in the surface relaxation, while the relaxations of these surface atoms are denoted by black arrows.

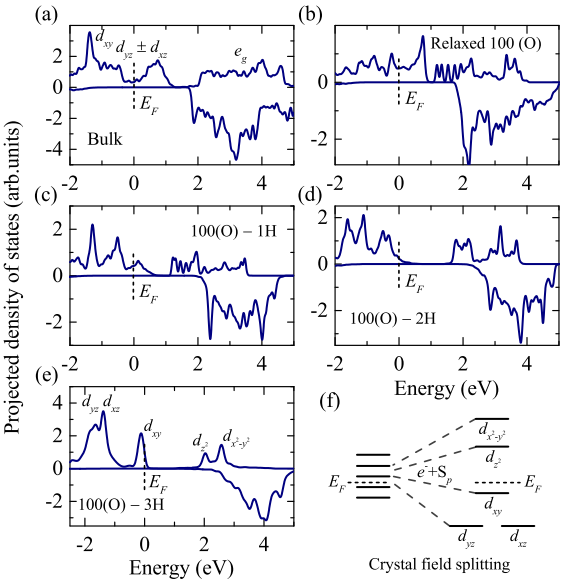


FIG. 3. Spin-polarized projected density of states calculated for (a) bulk $CrO_2$ and the surfaces of (b) ideal 100(O), and LCCs-participated (c) 100(O)–H, (d) 100(O)–2H, and (e) 100(O)–3H. The Fermi levels are set to zero, as indicated by the vertical dash lines; (f) an illustrated diagram for HF–SmC transition on 100(O) surface.

### B. The O deficient surface

At early time, some experiments tended to attribute the spin depolarization behavior, that is, the HM–SmC transition of the $CrO_2$ surface, to the intrinsic surface defect, as a result of the oxygen deficiency ambient [19,21]. In this regard, we believe it is to a large extent unlikely, for the surface defects to be the reason. Consider, for example, the oxygen reduced surface, which is the most favorable surface under this condition. For 100(O) surface, the removal of the top O atom leaves behind with one Cr atom, and the resultant structure is much equivalent to that of the 100(Cr) surface. As we will show later, the ideal 100(Cr) surface is not SmC either, in good agreement with an early study from DFT perspective [18]. Therefore the broken HM surface states observed cannot be understood in terms of the defect-driven surface reconstruction.

### C. The LCCs-participated surface

However, it is possible for there to be a distribution of local charge carriers (LCCs) on the $CrO_2$ surface. Such carriers are generally localized on the surface and may not be got rid of or compensated spontaneously [11–16], and hence may play an important role in determining the very realistic electronic and magnetic structures of the surface. These LCCs can be the isolated H atoms, group VII anions, or group IA ions, etc., that introduced unintentionally from, for example, the precursors in the sample growth or possible contaminations upon sample transfer. In particular, the commonly used $CrO_3$ precursor in CVD growth is extremely hygroscopic and easily contaminated [13,20], which make it behave as a possible LCCs trapper on the surface. Unlike surface defects, these charge carriers may not change the surface symmetry/coordination such drastically as the surface defects did and, in turn, will to a larger extent preserve the inherent crystal-field-symmetry of the surface, probably leading to surface characteristics substantially distinct from the above ideal/defective ones.

*Possible locations of LCCs on the 100(O) surface*. To ascertain how the LCCs could affect the surface morphology and electronic structure whereby fully understand the associated mechanism and the underlying physics, we now consider the isolated H atom as a typical example of the LCCs to deal with the problem. We first considered the 100(O) surface, and then extended this model to other (100) surfaces. For the 100(O) surface stemming from rutile $CrO_2$, there are up to four possible positions that can host the isolated LCC H in terms of chemical bindings, namely, (i) one site along the dangling bond vector of the first layer O, and (ii) one along the dangling bond vector of the second layer Cr, (iii)–(iv) two sites along the Cr–O plane normal with respect to the third layer and fourth layer O, respectively. Note that upon geometric relaxations, the LCC H will deviate more or less from their initial positions, in order to optimize the total electrostatic energy in terms of Columbic interactions, as shown in Figs. 2(b)–2(d). In accordance to our calculation, the bonding of H–Cr is much weaker than that of H–O, with the binding energy being a few eV of magnitude lower than the latter. So we can rule out the possibility of case (ii), and overall the $(1 \times 1)$ 100(O) surface can accommodate up to three LCC H in terms of H–O binding.

*The electronic structures*. The electronic structures of these LCCs-distributed surfaces were depicted in Figs. 3(c)–3(e). As the LCC is continuously introduced, the itinerant $t_{2g}$ states will behave more localized shifting down to lower energy and, eventually, situate below the Fermi level, as shown in Figs. 3(c)–3(e). This suggests that accompanied with the breaking of the double-exchange character, the system will experience a HM–SmC transition hereby breaking the HM surface state with the participation of a certain amount of LCCs. To explicitly understand the physics underlying this transition, in the following, we will specifically discuss the roles of these LCCs in the evolution of the surface state.

(i) *The protection of the crystal-field symmetry on the surface*: while it is remarkable noting from Fig. 2(a) that the relaxed 100(O) surface is subject to a distorted fivefold $Cr–O_5$ $S_p$ structure, the intervention of the LCC H [shown in Figs. 2(b)–2(d)] will gradually give rise to a recovery of the $S_p$ symmetry from such distortion and, in turn, give a more regular crystal-field splitting (CFS) of the surface Cr, as supported by the calculated PDOS of the 100(O)–3H surface shown in Fig. 3(e). Under the $S_p$ symmetry, the $3d$ states of the surface Cr are splitted into the lower-lying $d_{yz}$, $d_{xz}$, together with the higher-lying $d_{xy}$, and $d_{z^2}$,$d_{x^2-y^2}$ as well, much more regular than the broadening and small peaks in the relaxed 100(O) case, as indicated in Fig. 3(b).

(ii) *The electronic occupation of the majority-spin states and the exchange-coupling mode*: along with the regularization of CFS on the surface, the $t_{2g}$-like states (herein $d_{yz}$, $d_{xz}$, and $d_{xy}$) are gradually becoming fully occupied, with the electrons contributed from the $(O–H)^-$ pairs, which also converts the $CrO_2$ surface (from a double-exchange ferromagnet) into a superexchange magnet (to be discussed latter). We note that the formation of each $(O–H)^-$ pair will favorably denote one electron to the Cr atoms nearby, and due to the moderately itinerant character of the $t_{2g}$ states at the surface, such electron-donor states can effectively broaden to the second Cr layer

(the fifth atomic layer). Thus, from this point of view, the majority-spin $t_{2g}$ states of the surface would be fully occupied with participation of two $(O–H)^-$ pairs. However, the calculated PDOS in Fig. 3(d) suggest slightly different that for such case there remains a minor tail state of the $t_{2g}$ manifold lying above the Fermi level. This can be understood as a consequence of the distortion of the Cr–$O_5$ $S_p$ symmetry due to one missing surface O. Such tail state vanishes as the intervening of a third H, which can further restrain the Cr–$O_5$ $S_p$ distortion [see Fig. 2(d)] whereby yielding a SmC state with a gap of ∼2 eV edged by $t_{2g}$ and $e_g$ states, as displayed in Fig. 3(e).

(iii) *The rotation of* Cr–$O_5$ $S_p$: along with the restrained Cr–$O_5$ $S_p$ distortion, a rotation of the surface Cr–$O_5$ $S_p$ (which behaves as an ensemble) takes place, as typified in Figs. 2(c)–2(d). One of the bond bridging the third layer O and the fifth layer Cr is elongated, while the fourth layer O atom relaxes to the [−1−1 0] direction, altogether leading to a (clockwise) rotation of the surface Cr–$O_5$ $S_p$. It deserves our attention that such rotation will offer a large tendency for the O atoms undergoing a coordination conversation with respect to the neighboring Cr, in order to form a $Cr_2O_3$ phase, in which the O atoms are fourfold coordinated. Therefore it is evident that such rotation could be one of the driven factors account for the observed $CrO_2 \rightarrow Cr_2O_3$ transition on the surface. It should be pointed out that, since the LCC model is subject to a local regime, to break the HM surface state it is less necessary for there to be an overall coverage of LCCs on the surface sample. As we will show later that, the isolated LCCs will aggregate spontaneously on the surface in order to lower the energy. As a consequence, the Cr–$O_5$/Cr–$O_6$ rotation is likely to first take place in some local regions and then drive the HM–SmC transition broadening in larger areas.

## IV. THE SURFACE STATES OF OO-TERMINATED $CrO_2$ (100) SURFACE

### A. The clean surface

To further our understanding, we then moved our attention to the 100(OO) surface, as shown in Fig. 4, which was reported to be energetically even more stable than the 100(O) surface under O-rich conditions [32]. As mentioned above, the 100(OO) surface has three O dangling bonds, each carrying $2/3\,e^+$, i.e., $2e^+$ in total, leading to a charge polarity on the surface that cannot be compensated spontaneously. Our calculated PDOS suggest that for such case the 3*d* states of the surface Cr turned to be almost unoccupied, with the $t_{2g}$ and $e_g$ states shifting up higher, lying above the Fermi level, as depicted in Fig. 5(a), yielding a SmC state along with a charge transfer from the $t_{2g}$ states to the surface O dangling bonds. Note also form Fig. 4(a) that the surface Cr moves substantially upward to the topmost O in order to facilitate this charge redistribution.

*The reason for the instability of 100(OO) surface.* Although it is shown that the 100(OO) surface exhibits a SmC state, such state cannot be energetically stable (to be discussed later) or physically compatible to explain the experimentally observed SmC feature (in terms of $Cr_2O_3$), with the reason summarized as follows. (i) Due to the limited metallicity of Cr and as such a sixfold $O_h$ coordination, the constraint of the surface Cr to have

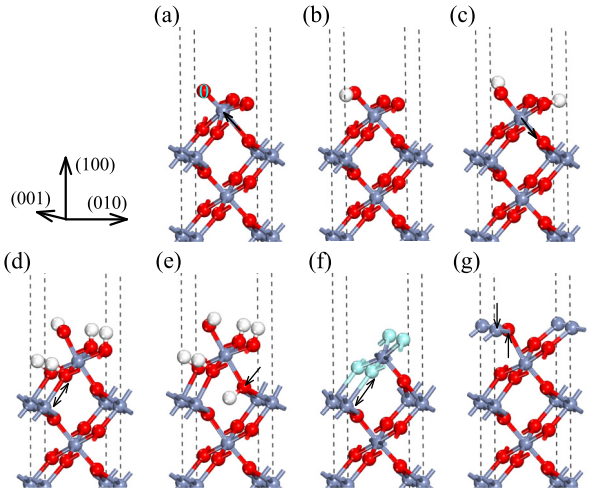


FIG. 4. The calculated surface geometries for the relaxed (a) 100(OO), (b) 100(OO)–H, (c) 100(OO)–2H, (d) 100(OO)–3H, (e) 100(OO)–4H, (f) 100(O)–$2F_O$, and (g) 100(Cr) surfaces. The arabic numeral 0 labels the additional O atom on 100(OO) surface, with respect to the 100(O) configuration. The relaxations of the surface atoms, when significant, are indicated by the black arrows.

a higher valency (+6) will drive the system into a $t_{2g}$-excited state. As we can see from Fig. 5(a), such unoccupied $t_{2g}$ states are not sufficiently high above the Fermi level, and therefore still play non-negligible roles in the exchange interaction as well as the inherent bonding behavior at the surface. (ii) Although the charge transfer between the surface Cr and

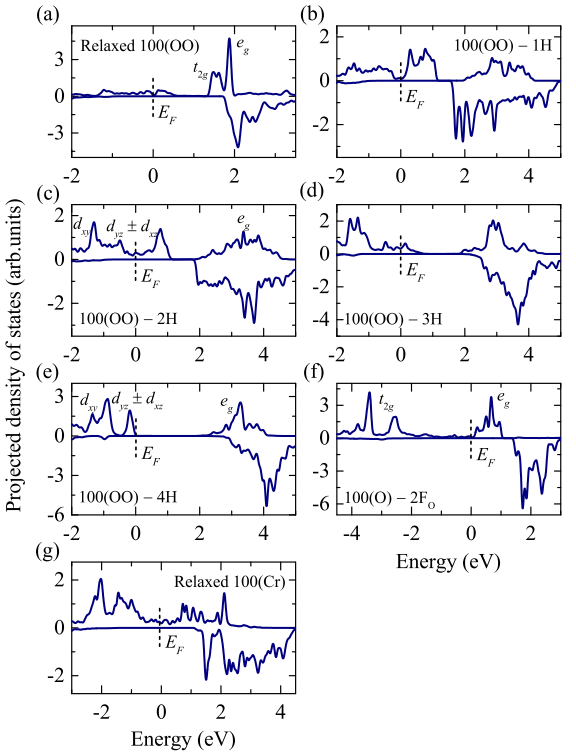


FIG. 5. Spin-polarized projected density of states calculated for relaxed (a) 100(OO), (b) 100(OO)–H, (c) 100(OO)–2H, (d) 100(OO)–3H, (e) 100(OO)–4H, (f) 100(O)–$2F_O$, and (g) 100(Cr) surfaces. The Fermi levels are set to zero, as indicated by the vertical dash lines.

O compensates the charge polarization of the surface dangling bonds, the underlying surface *charge polarity* retains. (iii) The breaking of the Cr–$O_6$ $O_h$ symmetry at the surface due to the distortion of the surface Cr, which has a close association with the CFS, should be taken into account here as another reason.

### B. The LCCs-introduced surface

*The 100(OO)-2H surface*. Given the surface character of the 100(OO), we shall next examine the evolution of the surface states as the interference of LCCs. The 100(OO) surface has one more surface O than the 100(O), and hence is able to accommodate one more LCC, i.e., up to four LCCs. The first two LCCs are expected to favorably exhibit a charge balance between the surface $Cr^{6+}$ and $O^{2-}$ and in turn, lead to a charge-neutral $(Cr^{4+}–2O^{2-})^0$ state. Such state is comparable to the surface state of the 100(O) in the sense of surface charge population, as in the latter case the surface dangling bonds are compensated spontaneously with the assistance of atomic relaxations, and this is further verified by the calculated PDOS shown in Figs. 5(b)–5(c): the $t_{2g}$ state of the 100(OO) surface is gradually becomes occupied, converting the $Cr^{6+}$ into a $Cr^{4+}$ state with the participation of two LCCs.

However, there remains a slight difference being that the CFS of the surface Cr here is much more regular than the case of the relaxed 100(O), and even *much comparable* to that in the *bulk* $CrO_2$: the $t_{2g}$ state is isolated into the lower-lying $d_{xy}$ state together with the higher-lying $d_{xy\pm yz}$ states, as verified in Figs. 5(c) and 3(a). The reason can be understood as follows: while the 100(O) surface is subject to a $S_p$ symmetry in which the Cr is fivefold coordinated with one missing O, the 100(OO) surface has a $O_h$ symmetry much comparable with the CF symmetry in the bulk, where the Cr is sixfold coordinated; on the other hand, as the introducing of LCC H, the distortion of the surface Cr of 100(OO) is also substantially suppressed. The distorted Cr atom relaxes backward to the center of the Cr–$O_6$ octahedron as shown in Figs. 4(a)–4(c). Therefore the first two LCCs play an important role in the recovery of the CF symmetry of 100(OO) surface from such distortion and, in turn, stabilize the surface electronic structure.

*The 100(OO)-4H surface*. On the basis of the above fact, the introduction of additional two LCCs will favorably convert the HM surface into a SmC state, as shown in Figs. 5(d)–5(e). In line with the 100(O)–2H case, a rotation of the Cr–$O_6$ $O_h$ (clockwise) also takes place on 100(O)–4H surface to drive the HM–SmC transition. However, slightly different from the 100(O)–2H case where a tail state is to be observed around the Fermi level, the 100(OO)–4H surface does not exhibit such a tail state, owing to the coordination number and the CFS both distinct from the former ones. To further verify this difference, we have considered a different type LCC, i.e., the substitution of F atom on the surface O ($F_O$), to be introduced onto the 100(O) surface instead of H. Indeed, the calculated result indicates an HM–SmC transition accompanied by a flat tail state as shown in Fig. 5(f), despite that F is a strong oxidant, in line with the 100(O)–2H case.

### C. The 100(Cr) surface

Here, one would also argue that for the 100(Cr) surface (O-reduced), which has 3 Cr dangling bonds each carrying 2/3 $e^+$, the surface charge state is right the same as that of 100(O)–2H or 100(OO)–4H case, but why could this surface remains half-metallic? [See Fig. 5(g)]. On this point, our results show that for the ideal 100(Cr) surface, the topmost Cr is isolated binding with three O atoms below. Upon the relaxation, the Cr atom will move downward and form a planer stage bonding with O, through a $sp^2$-like interaction. With such a surface configuration, the 3$d$ states of Cr are then isolated into several small broadening peaks without energy gap. This explains why the Cr-terminated surface can preserve the half-metallicity. The above results also elucidate that the surface states of $CrO_2$ are not only dependent on the LCCs, but are also strongly correlated to the coordination condition and the CFS, whereby suggesting the 100(O)–3H and 100(OO)–4H models to be strong candidates as the origin of the broken HM states observed on the $CrO_2$ (100) surface.

We should also point out that it is possible for the surface to have a distribution of fractional number O defect under O deficient conditions, i.e., removing from the surface (1–$x$) O instead of exactly *one* O atom. However, for such case, we considered that since the $O_{1-x}$ defective surface carries an overall charge density of state lower than (at least) $2e^-$ per (1 × 1) unit, which is essential for a SmC-surface-reconstruction as revealed in our study, the $O_{1-x}$ defective surface is unlikely to be SmC even more. This point is also in agreement with the view in Ref. [18], which elucidates that the surface with one missing O should be the ground-state configuration under O deficient conditions.

## V. THERMODYNAMIC STABILITY OF $CrO_2$ (100) SURFACE

The most straightforward way to check these models is subject to the calculation of their correlated surface thermodynamic stabilities. In this work, the surface energy of a LCC-free (100) surface is calculated in accordance to

$$2\sigma^{\rm surf}_{(100)} = E^{\rm slab}_{(100)} - n_{\rm O}\mu_{\rm O} - n_{\rm Cr}\mu_{\rm Cr}, \tag{1}$$

where $E^{\rm slab}_{(100)}$ is the total energy of the (100) surface slab, $n_{\rm O}$ and $n_{\rm Cr}$ are the numbers of O and Cr atoms contained in the slab, respectively, with $\mu_{\rm O}$ and $\mu_{\rm Cr}$ being the chemical potentials of O and Cr, which should follow the relation

$$2\mu_{\rm O} + \mu_{\rm Cr} = E^{\rm bulk}_{\rm CrO_2}. \tag{2}$$

The surface energy of the LCC-participated (100) surface is then calculated following the relation

$$\sigma^{\rm surf}_{(100)-n{\rm H}} + \sigma^{\rm surf}_{(100)} = E^{\rm slab}_{(100)-n{\rm H}} - n_{\rm O}\mu_{\rm O} - n_{\rm Cr}\mu_{\rm Cr} - n_{\rm H}\mu_{\rm H}. \tag{3}$$

Therefore

$$\sigma^{\rm surf}_{(100)-n{\rm H}} = E^{\rm slab}_{(100)-n{\rm H}} - \sigma^{\rm surf}_{(100)} - n_{\rm O}\mu_{\rm O} - n_{\rm Cr}\mu_{\rm Cr} - n_{\rm H}\mu_{\rm H}, \tag{4}$$

where $E^{\rm slab}_{(100)-n{\rm H}}$ is the total energy of a surface slab containing LCC H on the top, with $n_{\rm H}$ to be the number of this LCC, and $\mu_{\rm H}$ its chemical potential, which should fulfill the following limits, in order to prevent the formation of $H_2O$ and elementary

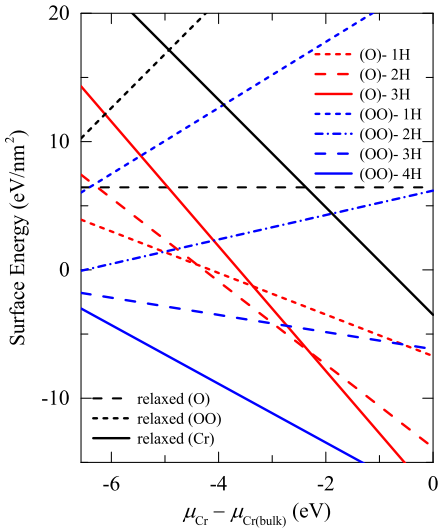


FIG. 6. Calculated surface energies of LCC-present $CrO_2$ (100) surfaces, as a function of $\mu_{Cr}$. For reference, the surface energies of three LCC-free surfaces are also given.

substance $H_2$ on the surface:

$$2\mu_H + \mu_O < E_{H_2O}, \quad (5)$$

$$2\mu_H < E_{H_2}, \quad (6)$$

where $E_{H_2O}$ and $E_{H_2}$ are total energies of the molecular $H_2$ and $H_2O$, respectively. Figure 6 depicts the surface energy of the LCC-present (100) surface, including 100(O)-$n$H ($n$ = 1, 2, 3) and 100(OO)-$m$H (m = 1, 2, 3, 4) as prototypical cases, with the LCC-free 100(O), 100(OO), and 100(Cr) surfaces also given for comparison.

### A. The clean surface

Among the three ideal (100) surfaces (LCC-free), the 100(O) surface has the lowest surface energy in the widest chemical potential range, in agreement with an early DFT study [32]. However, a minor discrepancy is that according to our LSDA+$U$ calculations, the 100(Cr) surface is more stable in energy than the 100(OO) one, as shown in Fig. 6, and this is inconsistent with Ref [32]. This distinction is most likely due to the different correlation terms between LSDA+$U$ and LSDA. In this regard, our results suggest that certainly the LSDA+$U$ determination can be more adequate to this study. First of all, from several experimental observations [19,21] and in combination with an early theoretical study [18], it is conclusive that the (100) surface of $CrO_2$ favors a Cr-terminated structure under O-deficient/Cr-rich conditions; on the other hand, as discussed above, the 100(OO) surface is charge polarized with a metastable $t_{2g}$ state that is almost unoccupied. In contrast, the 100(Cr) surface (O-deficient surface) has its charge state much comparable to 100(O)–2H or 100(OO)–4H surfaces, and favors a reconstruction whereby converting the isolated Cr atom into a Cr–O $sp^2$-like configuration. Therefore it is reasonable for the 100(Cr) surface to be more stable. The above results also indicate that a reasonable electron-correlation term is crucial to obtain a correct electronic structure and surface energy in such systems, in good agreement with the previous perspective [5].

### B. The LCC-present surface

For the LCC-present (100) surfaces, in general, their surface energies will undergo substantial lowering with the participation of LCCs. In particular, the 100(O)–2H has lower surface energy than the corresponding LCC-free case, with the energy minimum occurring at the Cr-rich conditions, and this is true among almost all the chemical potential range; while the 100(O)–3H surface has higher energy than the ideal 100(O) under O-rich condition but lower energy under Cr-rich condition, due to the subsistent charge overcompensation. Still, the third H atom plays a crucial role in the surface symmetry protection and accounts for the energy lowering (at Cr-rich condition). Remarkably, the 100(OO) surface, which has the highest energy among all the LCC-free cases, experiences a sustained energy lowering as the LCCs are introduced, and turns out to be energetically the most stable with the participation of 4 LCCs, among all the cases as shown in Fig. 6. This again confirms our assumption on the origin of the broken HM surface state, i.e., the SmC nature, thereby giving the 100(OO)–4H to be the most stable surface configuration, rather than the ideal 100(O), 100(Cr) [reduced 100(O)] ever reported in previous studies [18,32].

Based on the above discussions, a new insight into the general rules [33–36] on the thermodynamics and reconstructions of ionic crystal surfaces is then realized: to our common sense, for the 100(O) surface of Tasker's II type (or the 100(OO)–2H surface), in which the anion and cation dangling bonds are fully saturated whereby satisfying the surface charge nonpolarity condition, intuitively no reconstruction is expected and the surface could be naturally stabilized by means of finite atomic relaxation, as is indeed supported by Ref. [32]. However, based on our electronic structure calculations and in combination with the surface energies, such surfaces would not be the most stable as long as the LCC model is considered, despite the breaking surface nonpolarity in the latter case. Instead, the 100(OO)–4H surface is suggested to be the most stable due to the LCCs-induced electronic surface reconstructions converting the itinerant $t_{2g}$ manifold into its ground state. Therefore the surfaces of $CrO_2$ are stabilized undergoing electronic reconstructions that do not satisfy the surface reconstruction rules and, in turn, the physics of the SmC nature is captured.

From the above discussions, it is demonstrated that for transition-metal oxides like $CrO_2$ the common rules on the surface reconstruction are no more applicable. To judge the surface stability, it is therefore essential to consider the electronic surface reconstruction taking into account the stability of their *subvalence* states, e.g., the $t_{2g}$ states of Cr. To this end, we notice that the enhanced stability of the triply degenerated $t_{2g}$ manifold due to the LCCs-driven electronic reconstruction along with an inerratic CFS (also depend on the introduced LCCs) as typified by the 100(OO)–4H case, counteracts with the subsistent surface charge polarity and accounts for the overall surface stability. This provides strong evidence for the calculated energy difference between the 100(OO)–4H and 100(OO) surfaces (in view of different surface charge states), and that between 100(OO)–4H and 100(O)–2H, or

100(OO)–2H and 100(O) surfaces (in view of different surface symmetries and coordinations). Such rationale is not only helpful to understand why $CrO_2$, as a half-metal usually has a SmC surface under the experimental conditions, but also offers a pathway to modulate the surface states and the surface stability for realistic applications. It should be pointed out that since the LCC model is orientation *independent*, its application is not restricted to the (100) surface, but can be extended to surfaces of other orientations as well as to interfaces.

## VI. APPLICATION OF THE LCC-MODEL TO $CrO_2$–$TiO_2$ INTERFACE

The remaining issue to be addressed is the recently predicted QAH state in the $CrO_2$–$TiO_2$ interface [9]. Such state has never been experimentally observed either before or after this prediction, in spite of the fact that the $CrO_2$ film is usually epitaxially grown on the $TiO_2$ substrate. We therefore cast doubt on the realistic characteristic of this interface under the experimental growth conditions. To address this issue, we then applied our LCC model to deal with the issue. For the $(1 \times 1)$ interface of $CrO_2$–$TiO_2$, 2 LCCs were introduced, accordingly, onto the interface of $CrO_2$ side, analogous to the configurations in 100(O)–2H or 100(OO)–4H model. Our results show that the interface energy will be lowered by 0.8 eV/H atom, i.e., 1.6 eV in total, as the LCCs were introduced onto the $CrO_2$ side. In contrast, no such energy lowering is to be attained for introducing the LCCs onto the $TiO_2$ side, again confirming the validity of our LCC model. This is because, for $TiO_2$, there is no subsistent metastable $t_{2g}$ state as in $CrO_2$, and its $d$ shell is fully unoccupied situated much higher above the $E_F$. Therefore the surface-reconstruction rules [33–36] could still hold for $TiO_2$. On the basis of the $TiO_2$–$CrO_2$-2H model, we have recalculated the electronic band structure of this interface within the superlattice geometry as proposed in Ref [9], the results are shown in Figs. 7(a)–7(b). For the ideal (LCC-free) interface, our calculation indicates, in agreement with Ref [9], that a pair of Dirac points indeed appears around the $E_F$ in ($\Gamma$, $\pm$M) space, under the protection of $S_4$ and $M_\pm$ symmetry [illustrated in Fig. 7(c)]. As the LCCs intervene, the Dirac states are broken simultaneously with the band degeneracies lifted, which is shown in Fig. 7(b). The introduction of the LCC will lead to the Cr–$O_6$ $O_h$ rotation at the interface as the rotation observed on the surface, whereby breaking the $S_4$ and $M_\pm$ symmetry [see Fig. 7(d)], and hence the Dirac states. Furthermore, the calculated magnetic coupling strength on the interface is lowered (from a magnitude of more than 150 meV) to an order of few meV with the inclusion of LCCs, indicating a magnetic phase transition of the $CrO_2$ at the interface, i.e., from a strong double-exchange ferromagnet to a weak superexchange paramagnet. Therefore, even if the Dirac states could exist, the interfacial magnetic exchange field, as revealed in our study, is far from sufficient to break the time-reversal symmetry in order to achieve a QAH state at finite temperature.

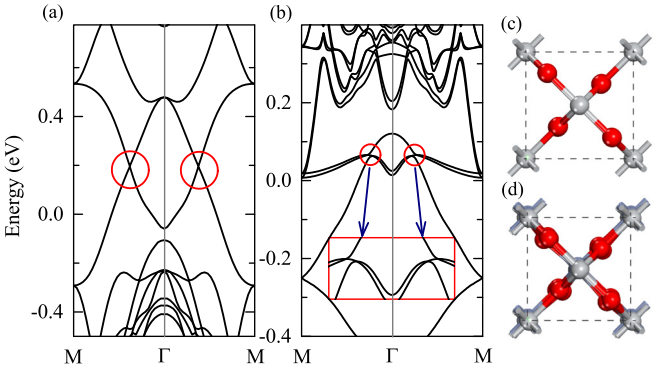


FIG. 7. Electronic band structures of (a) the ideal $TiO_2$ -$CrO_2$ interface and (b) $TiO_2$–$CrO_2$-2H interface, within a superlattice geometry as proposed in Ref [9]. The Dirac states [37] in the ideal interface are denoted by the red circles in (a), while the broken Dirac states, as a consequence of the LCCs, are indicated by the red circles in (b), whose scale is enlarged within a red block scheme. (c) The top view of $TiO_2$–$CrO_2$ interface with $S_4$ and $M_\pm$ symmetry. (d) Top view of $TiO_2$–$CrO_2$-2H interface, with broken symmetry (distorted O).

To preserve the HM characteristic of $CrO_2$ at the surface/interface, whereby taking full advantage of this material for spintronics applications or the purposes of the QAHE, here are some important guidelines for the experimental framework. (i) It would be advantageous to synthesize the surface/interface under O-rich/Cr-poor conditions, since the SmC surfaces normally have relatively lower energy and hence higher stability under Cr-rich condition; (ii) some unintentional local carriers, such as H, group VII anions, group IA ions, or other possible carrier providers (like aggregations of $OH^-$, $CO_3^{2-}$, etc.), should be to a large extent avoided; (iii) It might also be useful for the surface/interface samples to be annealed under O ambient conditions, in order to compensate the remaining LCCs such as H, via chemical reactions. This offers insight into why the HM surface states can be substantially enhanced upon annealing in O [19]; (iv) the surface/interface samples are suggested to be kept under O-rich ambient or ultrahigh vacuum/inert environment to restrain the intervention of the LCC.

## VII. CONCLUSIONS

In conclusion, in this study, we have probed the surface states of $CrO_2$ taking into account the intervention of some prototypical LCCs. In remarkable contrast to the ideal/O-reduced surfaces where a HM surface state was to be preserved, the LCCs can favorably drive the HM surface into a SmC state by means of an electronic surface reconstruction, thereby account for the experimentally observed spin depolarization and the metal-to-semiconductor transition on the surface and, hence, should be avoided. In particular, our study also elucidates that such electronic reconstruction does not fulfill the common surface reconstruction rules, and plays nonalternative roles with respect to the surface defect-driven reconstruction in the sense of surface stabilization and, in turn, offers a new insight into the general principle towards the surface thermodynamics and reconstructions. These findings not only provide strong evidence to interpret the reason underlying the not-yet-discovered QAHE in $CrO_2$–$TiO_2$ interface, but also offer a crucial step towards the full application of the HM surface states in spintronics and superconductors, and promote the realization of QAHE as well as other exotic properties in half-metal based systems.

**ACKNOWLEDGMENTS**

This work was supported by the NSF of China under Grant Nos. 11474145 and 11334003, the Nanshan Key Lab on Nonvolatile Memory (Grants No. KC2015ZDYF0002 and No. KC2015ZDYF0003A), the Shenzhen Fundamental Research Foundation (Grant No. JCYJ20170808153632616), and the Special Program for Applied Research on Super Computation of the NSFC-Guangdong Joint Fund (the second phase) under Grant No. U1501501. L.C. acknowledged the support of NSF of China under Grants No. 11474146 and No. U1532142; the Hong Kong, Macao, and Taiwan Science and Technology Cooperation Program of China (Grant No. 2015DFH10200); the NSF of Guangdong Province of China (Grant No. 2015A030310329); the Science and Technology Research Items of Shenzhen Grants No. JCYJ20160530185705301, and No. JCYJ20170412153325679 Support programs.

[1] M. I. Katsnelson, V. Yu. Irkhin, L. Chioncel, A. I. Lichtenstein, and R. A. de Groot, Rev. Mod. Phys. **80**, 315 (2008).
[2] J. M. D. Coey and M. Venkatesan, J. Appl. Phys. **91**, 8345 (2002).
[3] R. A. de Groot, F. M. Mueller, P. G. van Engen, and K. H. J. Buschow, Phys. Rev. Lett. **50**, 2024 (1983).
[4] K. Schwarz, J. Phys. F: Met. Phys. **16**, L211 (1986).
[5] M. A. Korotin, V. I. Anisimov, D. I. Khomskii, and G. A. Sawatzky, Phys. Rev. Lett. **80**, 4305 (1998).
[6] A. Singh, C. Jansen, K. Lahabi, and J. Aarts, Phys. Rev. X **6**, 041012 (2016).
[7] A. Singh, S. Voltan, K. Lahabi, and J. Aarts, Phys. Rev. X **5**, 021019 (2015).
[8] S. Voltan, A. Singh, and J. Aarts, Phys. Rev. B **94**, 054503 (2016).
[9] T. Y. Cai, X. Li, F. Wang, S. Ju, J. Feng, and C.-D. Gong, Nano Lett. **15**, 6434 (2015).
[10] R. Wang, Y. J. Jin, J. Z. Zhao, Z. J. Chen, Y. J. Zhao, and H. Xu, arXiv:1707.08899 (2017).
[11] K. P. Kämper, W. Schmitt, G. Güntherodt, R. J. Gambino, and R. Ruf, Phys. Rev. Lett. **59**, 2788 (1987).
[12] C. A. Ventrice, Jr, D. R. Borst, H. Geisler, J. van Ek, Y. B. Losovyj, P. S. Robbert, U. Diebold, J. A. Rodriguez, G. X. Miao, and A. Gupta, J. Phys.: Condens. Matter **19**, 315207 (2007).
[13] R. H. Cheng, B. Xu, C. N. Borca, A. Sokolov, C.-S. Yang, L. Yuan, S.-H. Liou, B. Doudin, and P. A. Dowben, Appl. Phys. Lett. **79**, 3122 (2001).
[14] C. F. Chang, D. J. Huang, A. Tanaka, G. Y. Guo, S. C. Chung, S.-T. Kao, S. G. Shyu, and C. T. Chen, Phys. Rev. B **71**, 052407 (2005).
[15] C. B. Stagarescu, X. Su, D. E. Eastman, K. N. Altmann, F. J. Himpsel, and A. Gupta, Phys. Rev. B **61**, R9233 (2000).
[16] R. K. Zheng, H. Liu, Y. Wang, and X. X. Zhang, Appl. Phys. Lett. **84**, 702 (2004).
[17] H. van Leuken and R. A. de Groot, Phys. Rev. B **51**, 7176 (1995).
[18] F. Hong and J. G. Che, Appl. Phys. Lett. **88**, 121903 (2006).
[19] Yu. S. Dedkov, M. Fonine, C. König, U. Rüdiger, and G. Güntherodt, Appl. Phys. Lett. **80**, 4181 (2002).
[20] K. Iwai, Y. Muraoka, T. Wakita, M. Hirai, T. Yokoya, Y. Kato, T. Muro, and Y. Tamenori, J. Appl. Phys. **108**, 043916 (2010).
[21] Yu. S. Dedkov, A. S. Vinogradov, M. Fonin, C. König, D. V. Vyalikh, A. B. Preobrajenski, S. A. Krasnikov, E. Yu. Kleimenov, M. A. Nesterov, U. Rüdiger, S. L. Molodtsov, and G. Güntherodt, Phys. Rev. B **72**, 060401(R) (2005).
[22] F. Hong and J. G. Che, Phys. Rev. Lett. **96**, 167206 (2006).
[23] G. Kresse and J. Furthmüller, Phys. Rev. B **54**, 11169 (1996).
[24] J. P. Perdew, K. Burke, and M. Ernzerhof, Phys. Rev. Lett. **77**, 3865 (1996).
[25] I. Solovyev, N. Hamada, and K. Terakura, Phys. Rev. B **53**, 7158 (1996).
[26] W. E. Pickett, S. C. Erwin, and E. C. Ethridge, Phys. Rev. B **58**, 1201 (1998).
[27] A. I. Liechtenstein, V. I. Anisimov, and J. Zaanen, Phys. Rev. B **52**, R5467(R) (1995).
[28] G. Kresse and D. Joubert, Phys. Rev. B **59**, 1758 (1999).
[29] L. Chioncel, H. Allmaier, E. Arrigoni, A. Yamasaki, M. Daghofer, M. I. Katsnelson, and A. I. Lichtenstein, Phys. Rev. B **75**, 140406 (2007).
[30] P. Schlottmann, Phys. Rev. B **67**, 174419 (2003).
[31] L. Craco, M. S. Laad, and E. Müller-Hartmann, Phys. Rev. Lett. **90**, 237203 (2003).
[32] J. J. Attema, M. A. Uijttewaal, G. A. de Wijs, and R. A. de Groot, Phys. Rev. B **77**, 165109 (2008).
[33] W. Harrison, J. Vac. Sci. Technol. **16**, 1492 (1979).
[34] P. W. Tasker, J. Phys. C: Solid State Phys. **12**, 4977 (1979).
[35] M. D. Pashley, Phys. Rev. B **40**, 10481 (1989).
[36] S. B. Zhang and S.-H. Wei, Phys. Rev. Lett. **92**, 086102 (2004).
[37] Slightly different from the band structures in Ref. [9] where a pair of Dirac cones were to be observed appearing exactly at the Fermi level, our results manifest that the Dirac states will deviate from the Fermi level by ∼0.2 eV. This discrepancy is likely due to different on-site Coulomb corrections considered for Cr 3*d* states, as in our study an intraorbital exchange potential *J* term has been applied. However, this minor difference will not change our conclusion to the problem.